TELKOMNIKA Telecommunication, Computing, Electronics and Control
Vol. 18, No. 2, April 2020, pp. 1062~1071
ISSN: 1693-6930, accredited First Grade by Kemenristekdikti, Decree No: 21/E/KPT/2018
DOI: 10.12928/TELKOMNIKA.v18i2.14282

Rogowski coil sensor in the digitization process to detect partial discharge

Eka Putra Waldi[1], Asri Indah Lestari[2], Rudy Fernandez[3], Syaifa Mulyadi[4], Yoshinobu Murakami[5], Naohiro Hozumi[6]
[1,2,3,4]Department of Electrical Engineering, Universitas Andalas, Indonesia
[5,6]Electrical and Electronic Information Engineering, Toyohashi University of Technology, Japan

Article Info

Article history:

Received Oct 6, 2019
Revised Dec 27, 2019
Accepted Feb 19, 2020

Keywords:

Back wire
Digitalization
Linearity
Partial discharge
Rogowski sensor

ABSTRACT

This paper presents the construction of a Rogowski Coil sensor with an air core to detect partial discharge using a digital oscilloscope. Two types of sensors are used. The first is the primary sensor winding with back wire, and the second is without back wire, labeled BW and WBW, respectively. The numbers of primary-turn in the sensors are 5, 10, 20, and 40 turns. The performance of the sensors is tested using two types of tests. First, the wave response test with a fixed imitation partial discharge magnitude input is used to select the optimum sensitivity with the lower sampling rate, aims to select the peak or valley value as a magnitude partial discharge value. The second test is using an imitation partial discharge ramp to check the linearity of the sensors. The imitation of the partial discharge inputs is generated by a commercial charge calibrator. The wave response test results show an increase in the number of turns that corresponds to an increase of the sensor output for both sensors in a non-linear trend. In determining the sampling rate, the detection of magnitude in the valley is better than the peak. All sensors act linear toward the imitation partial discharge ramp either in BW or WBW conditions.

Corresponding Author:

Eka Putra Waldi,
Department of Electrical Engineering,
Andalas University,
Kampus Limau Manis, Padang, West Sumatra 25163, Indonesia.
Email: ekawaldi@eng.unand.ac.id

1. INTRODUCTION

Partial discharge is one of the main mechanisms of aging, which leads to failure of catastrophic insulation in continuous operation. The asymmetrical configuration of the electrodes or the different types of insulating material creates an inhomogeneous electric field. An inhomogeneous electric field causes partial discharge. One example of the cause of the unevenness of the insulating material is the occurrence of air bubbles in solid insulation. The partial discharges occur in air bubbles, which results in continuous destruction of the surface leading to one side of the conductor, which means the distance of the conductor separator becomes smaller than before. Even with an increase in the frequency of PD can cause excessive heat, which results in increased destruction activity that occurs in propagation that forms a tree (treeing) like a conductor containing an electric charge due to PD to one of the more intense conductors. Treeing increases the strength of the electric field significantly, failing insulation [1-3]. Catastrophic insulation must be overcome if the detection of PD periodically to be detected early symptoms of aging insulation. A PD

produces a signal that has a short duration and small magnitude compared to the actual source voltage, so it needs a hardware (sensor) to detect it. There are two conventional ways of measuring PD. The first way is to connect the sensor in series with the sample. The disadvantage of this circuit is not safe against overvoltages when sample failure occurs. The second way is to connect the sensor in series with the capacitor, then connect it in parallel with the sample. The advantage circuit is safe against overvoltages when sample failure occurs [4-10]. The capacitor functions as a voltage divider and as a High Pass filter so that the sensor is safe against high voltage and only accepts high-frequency signals (PD signals). To be read by the measuring instrument, an amplifier is used so that the small-signal can be read by the acquisition device, and the digitization process requires adjusting the pulse width using an integrator method.

Today's technological sophistication, the digitization process has reached the level of Mega Sampling per second (MS/s) even to Giga MS/s and the smallest scale of millivolts. It allows reading partial discharge signals that have high frequency and low magnitude without using an amplifier. Induction Sensor is one of the high-frequency signal detection [11-14]. In addition, manufacturing sensors are economical compared to commercial sensors. One induction sensor that is widely used is the Rogowski coil sensor. Rogowski coil sensors have Primary and Secondary parts. The Primary section has one turn and functions as a signal receiver in the form of instantaneous current. The Secondary Section has several turns and serves to change the instantaneous current signal in the form Primary magnetic flux section to the Secondary section into a transient Voltage. The ends of the cable are returned to their original positions so that both ends of the cable are at the same point. The wire that returns to its initial position is named by Return Wire, whereas in this paper, it is called Back Wire [15-22]. In a single-phase measurement, there is usually no disturbing external flux, as well as a three-phase circuit that is symmetrically mounted. Then there is no disturbing outside flux. Furthermore, this study does not use Back Wire.

Many kinds of research discuss the response to sensors that are made even to the point of researching the matching impedance problems needed when an acquisition device is used. Until now, the discussion about the effect of the number of primary turns of the sensor has not been too detailed [22-24]. Furthermore, data acquisition also requires a characteristic of the wave to be read so that the use of a sampling rate can be determined. This research makes an economical sensor by paying attention to the accuracy of the acquisition by varying the number of secondary winding that has back wire (BW) and which does not have back wire (NBW). It is essential to test the sensor's capabilities compared to commercial sensors.

2. RESEARCH METHOD

In general, Rogowski's coil (RC) sensors work according to the laws of electromagnetic induction, where the instantaneous current through the primary winding conductor produces an instantaneous magnetic field in the form of magnetic flux that is directly proportional to the surface area that covers it. This flux induces a secondary winding conductor. Following Faraday's law related to induction by flux changes, the secondary winding produces an opposing flux, which is characterized by a potential difference between the ends of the secondary winding conductors. The voltage on the secondary winding is the result of the instantaneous current response detected. Where the voltage is proportional to the function of current changes with time. Mathematically, the resulting induced voltage can be expressed by:

$$E = M \frac{di_0}{dt} \tag{1}$$

where i_o is the instantaneous current of a PD pulse passing through the Primary part, which changes with time function, and M is the mutual inductance between the secondary part of the sensor loop and the Primary part.

$$M = NW \frac{\mu_0}{2\pi} \ln \frac{b}{a} \tag{2}$$

$$L = N^2 W \frac{\mu_0}{2\pi} \ln \frac{b}{a} \tag{3}$$

N is the turn number of the Secondary part, and the picture shows in Figure 1 (a). The following parameters are the geometrical construction (core) of the Rogowski sensor, W is the height of the sensor, a is the inside diameter of the sensor, and d is the outside diameter of the sensor [9], the picture can show in Figure 1 (b). The nonmagnetic material core in the form of polyethylene. The values of the parameters display Table 1. Variation of the number of turns and using a back wire (BW) for RC variations as Sample conditions expression in Table 2. All researchers agree that the equivalent circuit is the same shape [23],

the equivalent circuit can show in Figure 2. Sensitive sensors are carried out by linearity testing of input increases as shown in Figure 3. In this series, the function generator functions as a source and regulator of the amount of charge that is the input for the charge calibrator. Then the total charge is calculated by the formula:

$$Q = C\,V \tag{4}$$

Q is the magnitude of the charge simulation with units of pico coulombs (pC), C is a capacitor with a unit of farads (F), and V is the magnitude of the voltage application. A wave magnitude that produces PD represents a magnitude PD that calibrates with a charge calibrator.

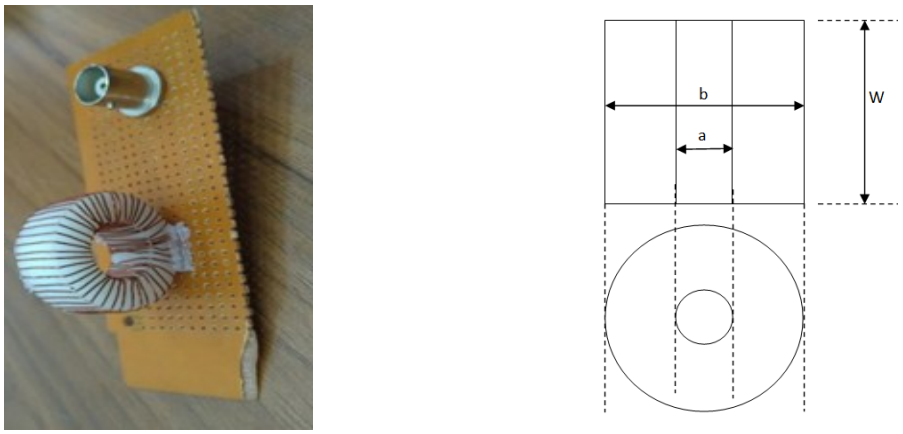

(a) (b)

Figure 1. (a) The RC sensor, (b) Coil dimension

Table 1. Geometrical parameters of the coil

Coil parameter	Symbols
Inside diameter	a
Outside diameter	b
Thickness	W

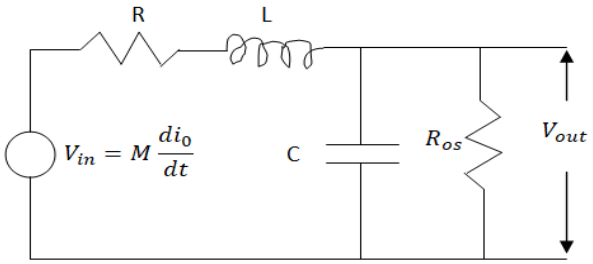

Figure 2. Equivalent circuit of RC sensor with oscilloscope

Table 2. Sample conditions

No.	Name of sample	Number of turns	Remarks
1	WBWN5	5	Without Back Wire
2	WBWN10	10	Without Back Wire
3	WBWN20	20	Without Back Wire
4	WBWN40	40	Without Back Wire
5	BW5	5	Back Wire
6	BW10	10	Back Wire
7	BW20	20	Back Wire
8	BW40	40	Back Wire

This study uses two types of samples with variations of the same number of turns. The first type of coil uses back wire and the second does not use back wire. The variation of the number of turns in each type of sensor is 5, 10, 20 and 40, as illustrated in Figure 4. The working principle of measuring the charge variation for the linearity test in Figure 3 is as follows. First, according to (4), the function generator (FG) can adjust the charge by determining the pulse voltage (V). The Output FG arrange for input to the charge calibrator (Haefely Type 9218 signal calibrator), the capacitor used is 141 pF.

Furthermore, determining the charge value is the multiplication voltage of the function generator with the capacitor used by the charge calibrator (CC) [25]. After that, the CC output gives the signal to the coupling capacitor (Haefely couling capacitor Type 9230). After that, the coupling capacitor in series with a commercial sensor (Haefly PD detector Type 9231) and RC sensor aims to compare the results of measurements on the same input. Response sensor measurements connect sequentially with Commercial and RC sensor output to the oscilloscope on channel-1 and channel-2. Labview program controls all measurement activity through a local area network (LAN) and storage of all digital data.

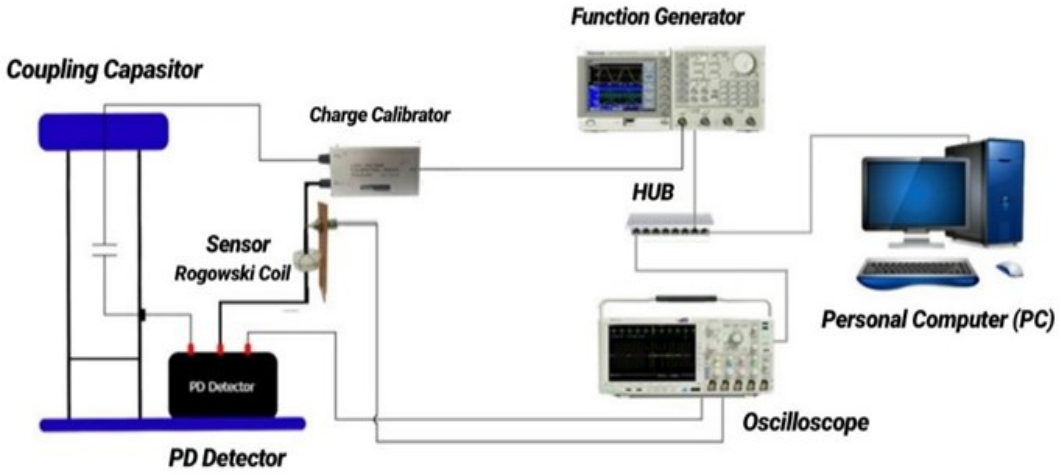

Figure 3. Linearity testing circuit for RC sensor

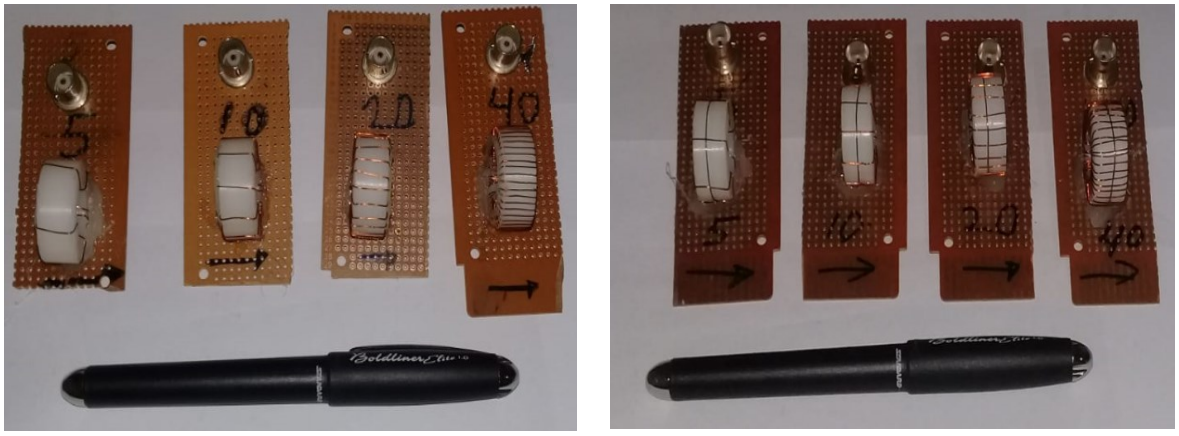

(a) (b)

Figure 4. RC sensors with the number of turns of 5, 10, 20, and 40: (a) without BW and (b) with BW

3. RESULTS AND ANALYSIS

Figure 5 is the measurement result of a standard sensor connected in series with the RC sensor with a different number of turns and given a back wire or not given a back wire. The amount of charge injected into the circuit is 705 pC and read by commercial sensors around 0.65 Volt. This figure shows that the wave up instantly with a span of 0.075 microseconds and instantly fell in 0.61 microseconds. Waveforms generated by commercial sensors such as critical damped or oscillation does not occur. Consequently, the peak value

set is visible. There is no effect on the number of secondary turns of the RC sensor on the PD significance read by the commercial sensor, nor is there any influence on the PD magnitude reading on sensors that have Back wire or do not have back wire. These results indicate that the measurement using the RC sensor does not interfere with the electrical activity that is taking place.

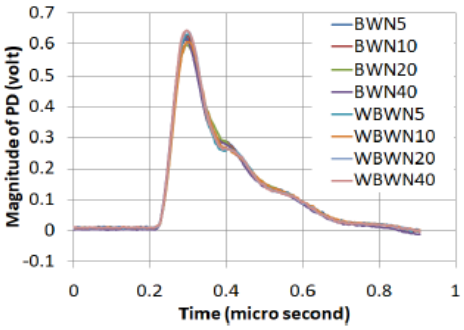

Figure 5. Effect of Commercial sensor output on RC sensors installed in series

Figure 6 (a) is a reading of commercial sensors and RC sensors that are given a back wire and are not given a back wire with a total of 40 turns. The result of the RC sensor response can be read directly by the oscilloscope well without using an amplifier, even though the magnitude that is read is much smaller than the commercial sensor response, it is shown in the picture in a dotted rectangular box. The waveforms produced by RC sensors are very different from commercial sensors, where the waveforms oscillate (underdamped). The measurement results of commercial sensors have larger than RC sensors. Thus, it is difficult to compare. Consequently, comparisons require a specific method.

Comparison of the characteristics of two waves using wave normalization by dividing the wave with its maximum value. Normalization shows that two waves have the same magnitude. The results show in Figure 6 (b). RC sensors respond to input signals earlier than commercial sensors, and RC wavelengths are shorter than commercial sensor waves. The output wave characteristics of the RC sensor are different from those of Commercial sensors. The results state that the RC sensor output oscillates concerning the time function while the commercial sensor does not oscillate, even though the oscilloscope uses an input impedance of 50 ohms (pure resistive) for which there is no capacitance value. The oscillation of the data informs that the RC sensor not only contains inductor and resistor but also contains capacitance [6], and there is no significant difference between RC sensors that are given BW or without BW, where the wave normalization in the two waves is the same shape.

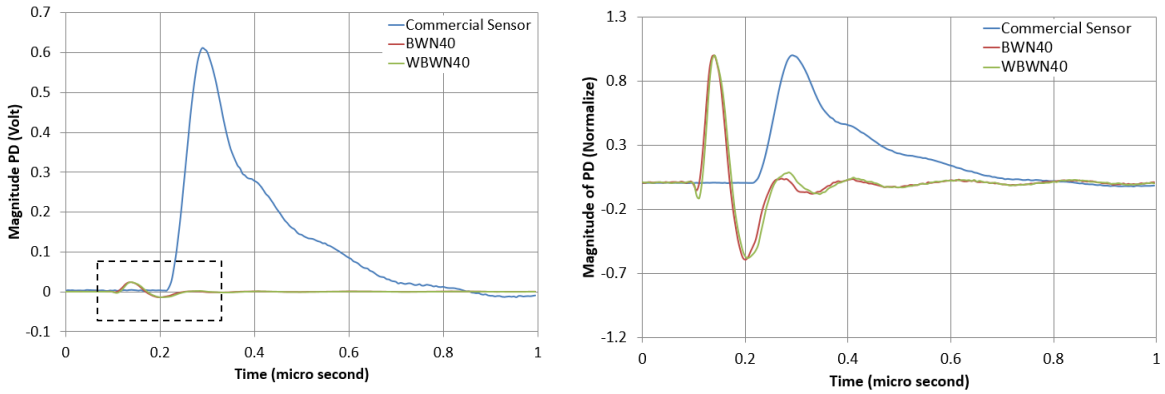

(a) (b)

Figure 6. (a) The response of all types of RC sensors, (b) Normalized wave response

Figure 7 is the result of measurements of each RC sensor with a different number of secondary turns. In Figure 7 (a) is the result of measuring RC sensors without using BW, and Figure 7 (b) is the result of measuring RC sensors using BW. The determination of the PD magnitude represented by the oscillating maximum wave amplitude has been defined at the dominant amplitude [15]. The results of the RC sensor measurements in Figure 7 illustrate that the positive amplitude is slightly different from the absolute value of the negative amplitude, as consideration for selecting that value as the peak value. Furthermore, in each RC sensor response, the amplitude of the positive and negative wave in Figure 7 (a) and Figure 7 (b), an absolute magnitude function of the number of turns can be developed into Figure 8. The information in the figure, where BWN (max) and WBWN (max) is the positive amplitude of each wave type, while BWN (min) and WBWN (min) is the absolute value of the negative amplitude of each wave type. The results show that generally, the amplitude increases when the number of turns is increased from 5 to 20 turns and remains even though the number of turns is increased to 40 turns. The BWN sensor has a greater magnitude compared to the WBWN sensor.

The absolute magnitude of the negative wave uses it as an alternative amplitude of PD magnitude. Thus it is necessary to calculate how much the percentage of the value decreases to the value of the positive magnitude wave. The calculation uses the data in Figure 8, which is a function of the number of secondary turns of the RC sensor. Comparisons made are WBWN (absMin) against WBWN (Max) and BWN (absMin) with BWN (Max).

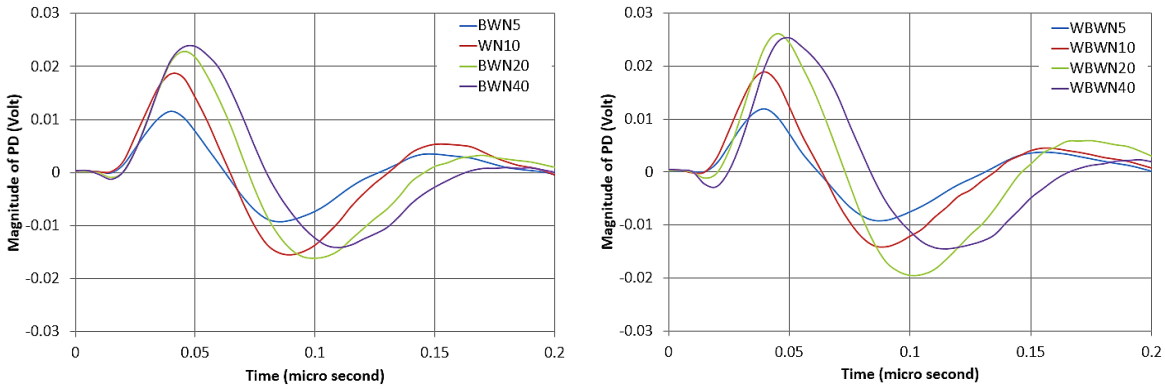

Figure 7. (a) Response Sensor on the variation of the number of turns with back wire, (b) Response Sensor on the variation of the number of turns without back wire

Sine or cosine waves are symmetrical waves, sampling the waves for the uncomplicated digitization process. The sampling rate of this wave is lower than the impulse wave. Impulse waves need little attention because the waves are of short duration with a duration above 90% peak located at no more than 10% of their period. That results in a sampling rate of peak detection of at least half the time of the wave peak period (Nyquist theorem). The magnitude of the sampling rate determines the accuracy of the peak value reading. The higher the sampling rate, the more accurate the peak value reading with the consequence requires a large amount of data [26]. Expectations require a technique for adjusting or changing the characteristics of the RC sensor in this study by varying the number of primary turns to change the sensor characteristics.

The input calculation from Figure 7 (a) and 7 (b) produces the output in Figure 9, and the calculation is a function of the number of turns, where the calculation use reference 26. The main vertical axis places the output on the left side with a left direction sign. BWN (Max) and WBWN (Max), in the number of turns 5 and 10, both have the same sampling rate with the value of 65 MS/s and a decrease to a value of 50 MS/s on the number of turns 20 and 40. BWN (absMin) sampling rate decreased from 40 to 33 MS/s when the number of turns increased from 5 to 10 turns. After that, it remained at 33 MS/s even though the number of turns increased to 40 turns. The WBWN (absMin) sampling rate decreases from 40 to 33 when the number of turns increases from 5 to 10 turns and continues to decrease up to 29 MS/s when the turns become 20 turns, after that, it remains even though the number of turns is increased to 40 turns. WBWN (DecMin) is the percentage of reduction in WBWN (absMin) to WBWN (Max), and BWN (DecMin) is the percentage of reduction in BWN (absMin) to BWN (Max) which is the output function of the number of turns. The graph puts the output on the secondary vertical axis and gives directions to the right in Figure 9. In general, the two data states an increase occurs if the number of turns increases.

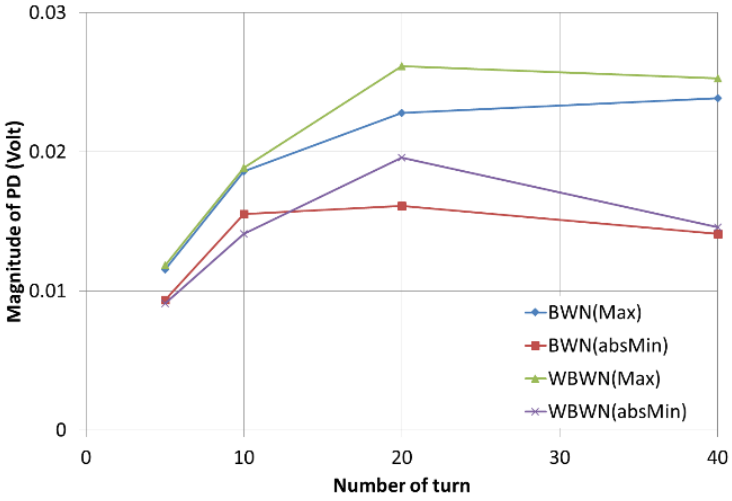

Figure 8. Magnitude PD depends on the number of turns in both polarities

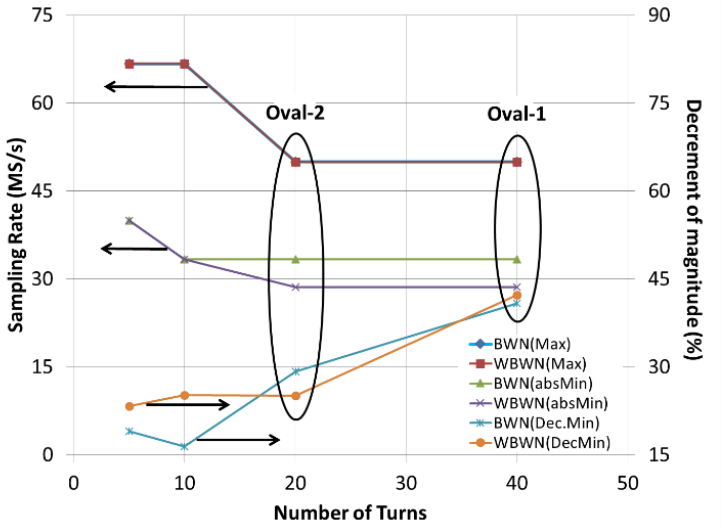

Figure 9. Sampling rate function of the number of turns and the decrement of the magnitude function of the number of turns and Decrement of magnitude depending on the number of turns

Reviewing the overall data are two essential things. There are two oval shapes added to graph 9 which are named Oval-1 and Oval-2. Oval-1 demonstrates the lowest sampling rate at WBWN (absMin) and BWN (absMin) although there is a slight difference in the value of the lowest sampling rate between WBWN (absMin) and BWN (absMin). Whereas the highest sampling rate is at WBWN (Max) and BWN (Max) with 40 turns. Oval-2 demonstrates the same sampling rate as Oval-1 but Oval-2 has a smaller number of turns than Oval-1, which is 20 turns and WBWN (DecMin) has a decrement of magnitude smaller than BWN (DecMin).

Figure 10 is the result of the sensor linearity test for the partial discharge imitation input. Figure 10 (a) is a sensor that uses a back wire while Figure 10(b) is a sensor that does not use a back wire. Both images illustrate that the sensor is linear with respect to the input of either positive or negative waves. These results state that the two types of sensors made qualify as a partial discharge measurement tool. Furthermore, the selection of the method to be used is in accordance with reference 26 where the acquisition data is able to read a peak value of 90% and is followed by the sensitivity of the equipment. When linked to Figure 9 the recommended reading is the smallest sampling value with a reading error of positive value of no more than 30%.

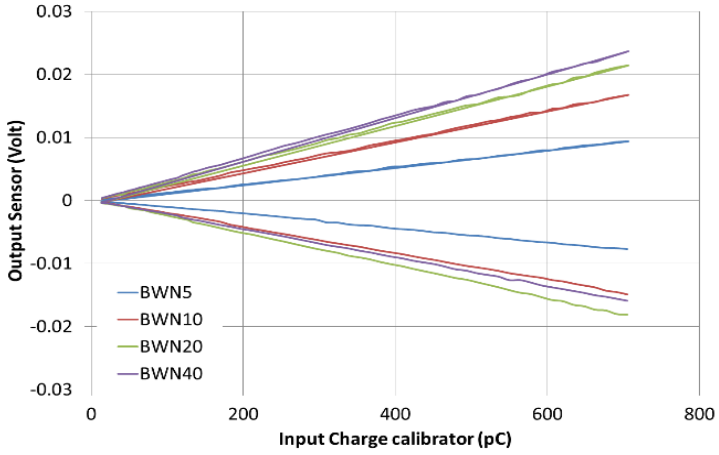

(a)

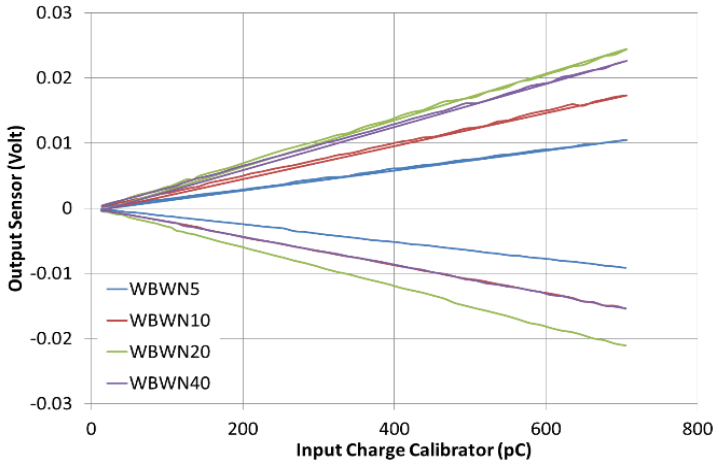

(b)

Figure 10. (a) Linearity test in the form of a sensor output function from the input charge calibrator on BWN, (b) on WBWN

4. CONCLUSION

The creation of the Rogowski sensor for detecting PD has been well-reviewed. Under the specific conditions described in this article with the following conclusions: (a) the wave response test results show an increase in the number of turns that corresponds to an increase in the sensor output for both sensors in a non-linear trend, but sensors act linear toward the imitation PD ramp; (b) PD reading technique with a sampling rate method is very effective reading on negative waves, where the smallest sampling rate is found on these waves.

ACKNOWLEDGMENTS

This research was supported by Direktorat Riset dan pengabdian Masyarakat direktorat Jendral penguatan Riset dan Pengembangan Kementrian Riset, Teknologi dan Pendidikan Tinggi. Following the research contract number. Number: 051/SP2H/LT/DRPM/2019. The fiscal year 2019.

REFERENCES

[1] B. Du, et al., "Understanding Trap Effects on Electrical Treeing Phenomena in EPDM/POSS Composites," *Scientific Reports*, vol. 8, pp. 1-11, 2018.
[2] M. Cacciari, et al., "An approach to partial-discharge investigation by height-distribution analysis," *IEE Proceedings – Science, Measurement and Technology*, vol. 142, no. 1, pp. 102-108, January 1995.
[3] S. Bahadoorsingh and S. M. Rowland, "Investigating the influence of the lubricant coating on hypodermic needles on electrical tree characteristics in epoxy resin," *IEEE Transactions on Dielectrics and Electrical Insulation*, vol. 17, no. 3, pp. 701-708, June 2010.

[4] R. Bartnikas, "Detection of Partial Discharges (Corona) in Electrical Apparatus," *IEEE Transactions on Electrical Insulation*, vol. 25, no. 1, pp. 111-124, February 1990.
[5] A. G. Sellars, et al., "Calibrating the UHF Technique of Partial Discharge Detection using a PD simulator," *IEEE Transactions on Dielectrics and Electrical Insulation*, vol. 2, no. 1, pp. 46-53, February 1995.
[6] E. Gulski, "Computer-aided Measurement of Partial Discharges in HV Equipment," *IEEE Transaction on Electrical Insulation*, vol. 28, no. 6, pp. 969-983, December 1993.
[7] A. A. L. Neyestanak, et al., "Design and implementation of a computer system for partial discharge process and detection," *2008 IEEE Canada Electric Power Conference*, pp. 1-6, 2008.
[8] M. Hikita, et al., "Measurements of Partial Discharges by Computer and Analysis of Partial Discharge Distribution by the Monte Carlo Method," *IEEE Transactions on Electrical Insulation*, vol. 25, no. 3, pp. 453-468, June 1990.
[9] M. Hoof and R. Patsch, "Analyzing partial discharge pulse sequences-a new approach to investigate degradation phenomena," *Proceedings of 1994 IEEE International Symposium on Electrical Insulation*, pp. 327-331, 1994.
[10] J. A. Hunter, et al., "Comparison of two partial discharge classification methods," *2010 IEEE International Symposium on Electrical Insulation*, pp. 1-5, 2010.
[11] M. Shafiq, et al., "Effect of geometrical parameters on high-frequency performance of Rogowski coil for partial discharge measurements," *Measurement*, vol. 49, no. 1, pp. 126-137, March 2014.
[12] F. Álvarez, et al., "Application of HFCT and UHF sensors in on-line partial discharge measurements for insulation diagnosis of high voltage equipment," *Sensors*, vol. 15, no. 4, pp. 7360-7387, March 2015.
[13] D. A. Ward and J. L. T. Exon, "Using Rogowski coils for transient current measurements," *Engineering Science and Education Journal*, vol. 2, no. 3, pp. 105-113, June 1993.
[14] E. P. Waldi, et al., "Development of HFCT for partial discharge sensors," *IOP Conference Series: Materials Science and Engineering*, vol. 602, 2019.
[15] W. F. Ray and C. R. Hewson, "High-performance Rogowski current transducers," *Conference Record - IAS Annual Meeting (IEEE Industry Applications Society)*, vol. 5, pp. 3083-3090, February 2000.
[16] M. Argüeso, et al., "Implementation of a Rogowski coil for the measurement of partial discharges," *Review of Scientific Instruments*, vol. 76, no. 6, p. 065107, 2005.
[17] Y. Liu, et al., "A novel transient fault current sensor based on the PCB Rogowski coil for overhead transmission lines," *Sensors*, vol. 16, no. 5, May 2016.
[18] A. Z. Abdullah, et al., "Development of smart online partial discharge monitoring system for medium voltage power cable," *International Journal of Power Electronics and Drive Systems*, vol. 10, no. 4, pp. 2190-2197, December 2019.
[19] G. Crotti, et al., "Analysis of Rogowski coil behavior under non-ideal measurement conditions," *19th IMEKO World Congress*, pp. 876-881, 2009.
[20] M. J. Foxall, et al., "Development of a new high current; Hybrid 'Ferrite-Rogowski'; high frequency current transformer for partial discharge sensing in medium and high voltage cabling," in *59th International Wire & Cable Symposium*, pp. 1-5, 2010.
[21] P. N. Murgatroyd, et al., "Making Rogowski coils," *Measurement Science and Technology*, vol. 2, no. 12, pp. 1218-1219, 1991.
[22] P. Li, T. Liang, Y. Cheng, and L. Zhao, "High-Freguency Characteristic of Rogowski Coil," *TELKOMNIKA Indonesia. J. Electr. Eng.,* vol 10, no. 8, pp. 2209-2214, 2012.
[23] B. Paophan, et al., "Implementation of A Rogowski ' s Coil for Partial Discharge Detection," *2016 19th International Conference on Electrical Machines and System (ICEMS),* pp. 1-4, 2016.
[24] G. Robles, et al., "Identification of parameters in a Rogowski coil used for the measurement of partial discharges," *Conference Record – IEEE Instrumentation and Measurement Technology Conference*, pp. 1-4, June 2007.
[25] J. Havunen and J. Hallstrom, "Application of Charge-Sensitive Preamplifier for the Calibration of Partial Discharge Calibrators below 1 pC," *IEEE Transactions on Instrumentation and Measurement*, vol. 68, no. 6, pp. 2034-2040, June 2019.
[26] E. P. Waldi, et al., "An optimized method of partial discharge data retrieval technique for phase-resolved pattern," *TELKOMNIKA Telecommunication Computing Electronics and Control*, vol. 14, no. 1, pp. 21-28, March 2016.

BIOGRAPHIES OF AUTHORS

Eka Putra Waldi received his B.S degree from Sriwijaya University in 1997, M.Eng. degrees from the Toyohashi University of Technology, Japan, in 2004, and Ph.D. degrees From Andalas University in 2017. Since 1999, he has been a lecturer at the Electrical Engineering Department, Universitas Andalas, Padang, Indonesia. His research interests are High Voltage phenomena and electrical insulation phenomena.

Asri Indah Lestari was born in Palembang, 30 December 1997. She completed her undergraduate education in the electrical engineering faculty from 2015 to 2019. She received her S.T degree from Muhammadiyah University of Palembang, Indonesia, in 2019, and now she is conducting a master's at Andalas University, Indonesia.

Syaifa Mulayadi, his S.T degree from Bung Hatta University in 2004 and M.T degrees from Universitas Andalas 2014. Since 2014, a lecturer at Akademi Maritim Sapta Saputra Padang. Electrical Engineering Department. His research interests are Antenna Design.

Rudy Fernandez received his S.T and M.T degrees from Universitas Indonesia in 1997 and 2010, respectively. Since 1999, he has been a lecturer at Electrical Engineering Department, Universitas Andalas, Padang, Indonesia. His research interests are Electromagnetic devices and Antenna Design.

Yoshinobu Murakami (Member) received his B.S., M.S., and Ph.D. degrees from the Toyohashi University of Technology, Japan, in 1997, 1999, and 2002, respectively. From 2001 to 2003, he was an assistant professor at Nagano collage of technology, Japan. He was an assistant professor from 2003 to 2008 and a lecturer from 2008 to 2010 at the Toyohashi University of Technology, Japan, respectively. Since 2010, he has been an associate professor at the Toyohashi University of Technology. His research interests are the development of measurement and diagnosis systems for dielectric and electrical insulation phenomena.

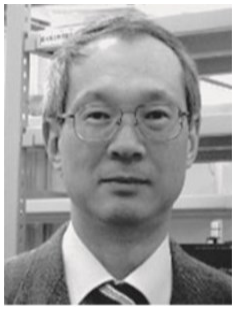

Naohiro Hozumi received his B.S. and M.S. degrees from Waseda University, Japan, in 1981 and 1983, respectively. From 1983 to 1999, he had joined the Central Research Institute of Electric Power Industry, Japan. He was an associate professor from 1999 to 2006 at the Toyohashi University of technology and a professor from 2006 to 2011 at the Aichi Institute of Technology, Japan, respectively. Since 2011, he has been a professor at the Toyohashi University of Technology. His research interests are insulating materials and diagnosis for high voltage equipment and measurement and signal processing for the medical device.